Inorg. Chem. **2008**, *47*, 10700−10707

Inorganic Chemistry
Article

Influence of Ligand Electronic Effects on the Structure of Monovalent Cobalt Complexes

Julie A. DuPont, Glenn P. A. Yap, and Charles G. Riordan*

Department of Chemistry and Biochemistry, University of Delaware, Newark, Delaware 19716

Received May 5, 2008

The syntheses, spectroscopic properties, and structures of the monovalent cobalt complexes, [PhTt^{tBu}]Co(L), **1-L** {PhTt^{tBu} = phenyltris[(*tert*-butylthio)methyl]borate; L = PPh_3, PMe_3, PEt_3, PMe_2Ph, $PMePh_2$, $P(OPh)_3$, $CNBu^t$}, are described. Complexes **1-L** are prepared via the sodium amalgam reduction of [PhTt^{tBu}]CoCl in the presence of L. The complexes display magnetic moments and paramagnetically shifted ^{1}H NMR spectra consistent with triplet, $S = 1$, ground states. The molecular geometries, determined by X-ray diffraction methods, reveal that some of the complexes display structures in which the L donor is moved off of the inherent 3-fold axis. In the most extreme cases (e.g., **1-P(OPh)$_3$** or **1-CNBu^t**), the geometries can be described as cis-divacant octahedra. The origin of the geometric distortions is a consequence of the electronic characteristics of L as first deduced by Detrich et al. for [Tp^{Np}]Co(L) (*J. Am. Chem. Soc.* **1996**, *118*, 1703). The results establish a linear correlation between the magnitude of the structural distortion and the electronic parameter of the phosphine donor.

Introduction

The development of monovalent cobalt complexes supported by the tris(thioether) ligand [PhTt^{tBu}] {PhTt^{tBu} = phenyltris[(*tert*-butylthio)methyl]borate} was motivated initially to provide benchmark complexes with which to compare the monovalent nickel complexes, [PhTt^R]Ni(L).[1] In the latter studies, we demonstrated that [PhTt^R]Ni(CO) (R = Bu^t, Ad) reacts with dioxygen yielding discrete, thermally sensitive adducts. Specifically, oxygenation of [PhTt^{tBu}]Ni(CO) resulted in the interception of the purple bis-μ-oxo dinickel(III), [(PhTt^{tBu})Ni]$_2$(μ-O)$_2$.[2] Alternatively, addition of dioxygen to [PhTt^{Ad}]Ni(CO) stopped at the 1:1 adduct formulated as Ni^{2+} superoxo, [PhTt^{Ad}]Ni(O_2), based on its electron paramagnetic resonance (EPR) and Ni X-ray absorption spectroscopy (XAS) characteristics as supported by density functional theory (DFT) results and reactivity studies.[3] More recent studies have extended chalcogen activation to sulfur; the reaction of [PhTt^{tBu}]Ni(CO) and S_8 produces the disulfido dinickel(II) complex, [(PhTt^{tBu})Ni]$_2$(μ-S_2).[4] Herein, we report the preparation and structural analyses of a series of monovalent cobalt complexes, [PhTt^{tBu}]Co(L) [L = PPh_3, PMe_3, PEt_3, PMe_2Ph, $PMePh_2$, $P(OPh)_3$, $CNBu^t$]. Some of these complexes display geometries wherein the donor ligand, L, resides far off of the inherent 3-fold axis (i.e., nonlinear B···Co−P angles). This structural phenom-

Scheme 1. Depiction of the α Angle as Defined by Theopold[5]

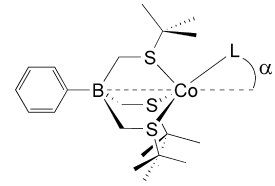

Scheme 2. Synthesis of Monovalent [PhTt^{tBu}]Co(L) from [PhTt^{tBu}]CoCl

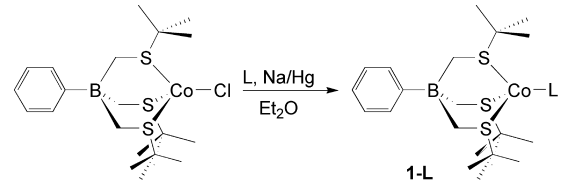

L = PPh_3, PMe_3, PEt_3, $PMePh_2$, PMe_2Ph, $P(OPh)_3$, $CNBu^t$

* To whom correspondence should be addressed. E-mail: riordan@udel.edu. Fax: 302-831-6335.

(1) Schebler, P. J.; Mandimutsira, B. S.; Riordan, C. G.; Liable-Sands, L. M.; Incarvito, C. D.; Rheingold, A. L. *J. Am. Chem. Soc.* **2001**, *123*, 331.
(2) Mandimutsira, B. S.; Yamarik, J. L.; Brunold, T. C.; Gu, W. W.; Cramer, S. P.; Riordan, C. G. *J. Am. Chem. Soc.* **2001**, *123*, 9194.
(3) Fujita, K.; Schenker, R.; Gu, W. W.; Brunold, T. C.; Cramer, S. P.; Riordan, C. G. *Inorg. Chem.* **2004**, *43*, 3324.
(4) Cho, J.; Van Heuvelen, K. M.; Yap, G. P. A.; Brunold, T. C.; Riordan, C. G. *Inorg. Chem.* **2008**, *47*, 3931.

10.1021/ic800813u CCC: $40.75
Published on Web 10/15/2008

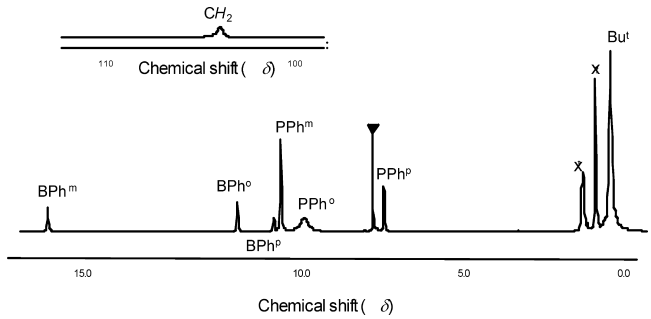

Figure 1. Proton NMR spectrum of [PhTt^{tBu}]Co(PPh$_3$) in C_6D_6 (▼). Residual pentane (×). Inset: δ 110−100 range.

enon was noted and described in detail by Theopold and Doren[5] for [Tp^{Np}]Co(L) complexes with π-acceptor ligands (i.e., L = N_2 and CO). In [Tp^{Np}]Co(CO), the CO ligand is 26.6° off of the 3-fold axis, where the deviation is defined as the α angle (Scheme 1), whereas in [(Tp^{Np})Co]$_2$(μ-N_2), α equals 34.7 and 37.8°. In this report, analysis of the structures of [PhTt^{tBu}]Co(L) as a function of the electronic properties of the phosphine ligands provides an understanding of the cobalt structural deviations complementing and extending significantly the examination of the two [Tp^{Np}]Co(L) complexes by expanding the observations to complexes possessing the [PhTt^{tBu}]Co fragment and to a systematic analysis of six phosphine donors.

Results

Ia. Synthesis of [PhTt^{tBu}]Co(L) [L = PPh$_3$, PMe$_3$, PEt$_3$, PMe$_2$Ph, PMePh$_2$, P(OPh)$_3$]. Under a nitrogen atmosphere, 1 equiv of the appropriate ligand L [L = PPh_3, PMe_3, PEt_3, PMe_2Ph, $PMePh_2$, $P(OPh)_3$] was added to a diethyl ether solution of [PhTt^{tBu}]CoCl and stirred, resulting in a color change from blue to green for L = PMe_3, PEt_3, PMe_2Ph, and $PMePh_2$; the addition of PPh_3 or $P(OPh)_3$ did not induce a color change. Subsequently, 1 equiv of a Na/Hg amalgam was added to the solution with vigorous stirring, resulting in a rapid color change from blue to pale green for L = PMe_3 and PEt_3 and from blue to yellow-green for L = PMe_2Ph and $PMePh_2$. For L = PPh_3, the solution color changed to yellow, and for L = $P(OPh)_3$, the solution changed to dark blue. Concomitant formation of a white precipitate was noted in all cases. Removal of the volatiles under reduced pressure, followed by extraction with pentane, afforded the corresponding monovalent cobalt species, **1-L**, in 40−66% isolated yields (Scheme 2). These thermally sensitive, high-spin, 16-electron complexes decompose rapidly upon exposure to air or moisture. The complexes are soluble in tetrahydrofuran (THF), ether, and pentane but react with chlorinated hydrocarbons (i.e., $CHCl_3$ or CH_2Cl_2) regenerating [PhTt^{tBu}]CoCl.

Ib. Proton NMR Spectroscopic Characteristics. The proton NMR spectrum of **1-PPh$_3$** is representative of the series of paramagnetic complexes (Figure 1). A broad singlet located downfield at δ 104.1 is assigned to the six methylene protons of the borato ligand. For this series of derivatives, the methylene proton chemical shifts range from δ 129.2 for **1-P(OPh)$_3$** to δ 55.2 for **1-PMePh$_2$**. A broad upfield resonance at δ 0.43 is assigned to the equivalent *tert*-butyl protons. A similar upfield shift was observed for the other **1-L** complexes with the *tert*-butyl proton resonances ranging from δ 0.60 for **1-PEt$_3$** to δ −7.51 for **1-PMePh$_2$**. The *meta*, *ortho*, and *para* protons of the borato ligand in **1-PPh$_3$** resonate at δ 16.2, 10.9, and 10.0, respectively. These assignments were made on the basis of signal integration and by assuming that the relative signal positions reflect a spin polarization mechanism. The *meta*, *ortho*, and *para* protons of the PPh_3 ligand were located at δ 9.76, 9.10, and 6.88, respectively. In the other **1-L** complexes, the phosphine protons were shifted significantly from values for the free phosphine. The proton NMR spectra of these cobalt(I) complexes are similar to those of the corresponding monovalent nickel species, [PhTt^{tBu}]Ni(L) (L = PMe_3, CO), synthesized previously in this laboratory.[1] The downfield shift of the methylene protons and the upfield shift of the *tert*-butyl protons of the borato ligand are comparable. The ^{31}P NMR spectra of the cobalt(I) complexes are devoid of signals, which is a consequence of efficient nuclear spin relaxation induced by the paramagnetic center. Similarly, Peters' [PhBP$_3$]Co(PR$_3$) derivatives do not display ^{31}P NMR signals.[6]

Table 1. Electronic Absorption and Room Temperature Magnetic Susceptibility Data for **1-PPh$_3$**, **1-PMe$_3$**, **1-PEt$_3$**, **1-PMePh$_2$**, **1-PMe$_2$Ph**, **1-P(OPh)$_3$**, and **1-CNBu^t**

	λ_{max}, nm (ϵ, M^{-1} cm^{-1})	μ_{eff}, μ_B
1-PPh$_3$	614 (30), 901 (596)	2.9(2)
1-PMe$_3$	686 (74), 893 (314)	3.1(1)
1-PEt$_3$	711 (135), 905 (671)	3.0(3)
1-PMe$_2$Ph	706 (70), 896 (508)	3.1(2)
1-PMePh$_2$	710 (49), 896 (618)	2.9(2)
1-P(OPh)$_3$	573 (120), 718 (257)	2.9(2)
1-CNBu^t	276 (235), 335 (192), 780 (17)	3.0(1)

The **1-L** complexes have triplet ground states, $S = 1$, as indicated by their bulk magnetic moments determined in solution by the Evans method. The values span a narrow range, $\mu_{eff} = 2.9-3.2\ \mu_B$, close to the spin-only value. [Tp^R][5] and [PhBP$_3^R$][6] ligated cobalt(I) complexes have similar magnetic moments.

The electronic spectra of the complexes **1-L** recorded in pentane (Table 1) display two optical bands consistent with a d^8 metal center in a pseudotetrahedral environment [i.e., analogous to the features found for tetrahedral nickel(II) complexes]. These transitions are consistent with similar Co(I) complexes, namely, [(Tp^{Np})Co]$_2$(μ-N_2) (λ_{max} = 783, 992 nm),[5] [PhBP$_3$]Co(PMe$_3$) (680 nm), and [(PhBP$^{iPr}_3$)Co]$_2$(μ-N_2) (745, 948 nm).[7] The two d-d optical transitions for the series of phosphine complexes range from λ_{max} (ϵ, M^{-1} cm^{-1}) = 711 (135) nm and 905 (671) nm for **1-PEt$_3$**, to 573 (120) nm and 718 (257) nm for **1-P(OPh)$_3$**. A rough correlation between the λ_{max} values of the higher-energy optical band and those of the electronic donor aptitude of the phosphine as defined by the Tolman electronic parameter is noted in

(5) Detrich, J. L.; Konecny, R.; Vetter, W. M.; Doren, D.; Rheingold, A. L.; Theopold, K. H. *J. Am. Chem. Soc.* **1996**, *118*, 1703.

(6) Jenkins, D. M.; Betley, T. A.; Peters, J. C. *J. Am. Chem. Soc.* **2002**, *124*, 11238.

(7) Betley, T. A.; Peters, J. C. *J. Am. Chem. Soc.* **2003**, *125*, 10782.

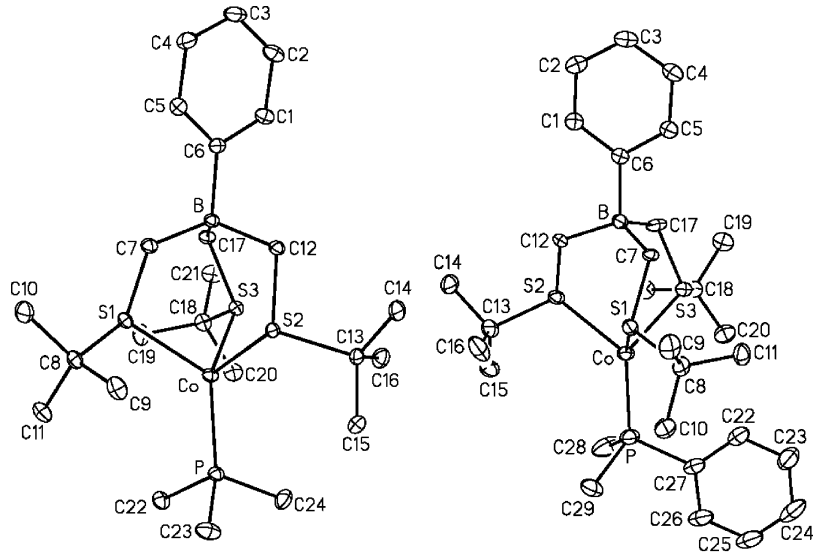

1-PMe$_3$ **1-PMe$_2$Ph**

Figure 2. Thermal ellipsoid plots of **1-PMe$_3$** and **1-PMe$_2$Ph** with atom labeling. Thermal ellipsoids are drawn to 30% probability. Hydrogen atoms have been omitted for clarity.

Table 2. Crystallographic Data for Complexes **1-PPh$_3$**, **1-PMe$_3$**, **1-PEt$_3$**, **1-PMePh$_2$**, **1-PMe$_2$Ph**, **1-P(OPh)$_3$**, and **1-CNBu^t**

	1-PPh$_3$	**1-PMe$_3$·2C$_6$H$_6$**	**1-PEt$_3$**	**1-PMePh$_2$·0.5C$_6$H$_6$**	**1-PMe$_2$Ph**	**1-P(OPh)$_3$**	**1-CNBu^t**
formula	$C_{39}H_{53}BCoPS_3$	$C_{36}H_{59}BCoPS_3$	$C_{27}H_{53}BCoPS_3$	$C_{34}H_{51}BCoPS_3$	$C_{32}H_{52}BCoPS_3$	$C_{39}H_{53}BCoO_3PS_3$	$C_{26}H_{47}BCoNS_3$
fw	718.70	688.72	574.58	656.64	633.63	766.70	539.57
cryst syst	monoclinic	monoclinic	monoclinic	triclinic	monoclinic	monoclinic	monoclinic
space group	*P*2(1)/*n*	*P*2(1)/*n*	*P*2(1)/*n*	$P\bar{1}$	*P*2(1)/*n*	*P*2(1)/*c*	*P*2(1)/*n*
a, Å	10.302(2)	9.676(2)	15.147(3)	13.644(3)	15.713(4)	10.667(2)	16.520(2)
b, Å	23.003(4)	24.678(5)	11.447(2)	15.072(3)	13.756(3)	17.983(3)	9.277(1)
c, Å	15.793(2)	16.249(3)	18.383(4)	17.226(3)	16.610(4)	20.792(4)	20.108(3)
α, deg	90	90	90	88.543(3)	90	90	90
β, deg	91.475(3)	94.471(3)	90.05(5)	86.444(3)	103.606(3)	97.251(3)	105.256(3)
γ, deg	90	90	90	84.079(3)	90	90	90
V, Å^3	3741.3(10)	3868.8(12)	3187.4(11)	3516.2(11)	3489.5(14)	3956.5(12)	3972.9(7)
Z	4	4	4	4	4	4	4
T, K	120	120	120	120	120	120	120
D_{calcd}, g cm^{-3}	1.276	1.182	1.197	1.240	1.206	1.287	1.206
2*θ* range, deg	1.77−28.29	1.65−28.24	1.11−21.99	1.18−28.32	1.94−28.28	1.92−28.32	1.85−28.31
μ(Mo Kα), mm^{-1}	0.695	0.669	0.799	0.733	0.736	0.667	0.802
R1, wR2[a]	0.0614, 0.1412	0.0419,0.1053	0.0912, 0.2176	0.0710,0.1928	0.0461, 0.1131	0.0386, 0.0879	0.0730, 0.1453

[a] Quantity minimized = $R(wF^2) = \sum[w(F_o^2 - F_c^2)^2]/\sum[(wF_o^2)^2]^1/_2$; $R = \sum\Delta/\sum(F_o)$, $\Delta = |(F_o - F_c)|$.

Table 1. The complexes with the most electron-releasing phosphines, **1-PMe$_3$** and **1-PEt$_3$**, have among the lowest-energy optical bands. Complex **1-P(OPh)$_3$**, with the electron-withdrawing phosphite, displays the highest-energy electronic transition. This trend is attributed, at least in part, to the change in orbital overlap that accompanies the geometry changes of the complexes. Specifically, moving the L donor off of the inherent 3-fold axis (i.e., increasing α angle values) increases Co-L *π*-orbital overlap, resulting in larger ligand field splitting and higher-energy optical transitions.

Ic. Molecular Structures of 1-PMe$_3$, 1-PEt$_3$, and 1-PMe$_2$Ph. The molecular structures of these three complexes, each containing electron-rich phosphine donors, are largely similar (Figure 2). Selected bond lengths and angles are contained in Tables 2 and 3. The common and most conspicuous structural feature is the nearly linear B···Co−P angle. The α angle equals 3.4, 1.7, and 1.0° for **1-PMe$_3$**, **1-PEt$_3$**, and **1-PMe$_2$Ph**, respectively. As a consequence, the P−Co−S angles are all quite similar averaging 123° for **1-PMe$_3$** and 124° for **1-PEt$_3$** and **1-PMe$_2$Ph**. The Co−S bond distances average 2.285, 2.302, and 2.306 Å for **1-PMe$_3$**, **1-PEt$_3$**, and **1-PMe$_2$Ph**, respectively. These distances are slightly shorter than those found in [PhTt^{tBu}]-Co(Me),[8] with an average Co−S bond distance of 2.35 Å.

Table 3. Selected Metric Parameters for **1-PMe$_3$**, **1-PEt$_3$**, and **1-PMe$_2$Ph**

		length, Å		angle, deg
1-PMe$_3$	Co−S(1)	2.2872(6)	B···Co−P	176.6(1)
	Co−S(2)	2.2845(6)	S(1)−Co−P	127.76(2)
	Co−S(3)	2.2841(6)	S(2)−Co−P	121.32(2)
	Co−P	2.2561(6)	S(3)−Co−P	120.23(2)
1-PEt$_3$	Co−S(1)	2.293(4)	B···Co−P	178.3(1)
	Co−S(2)	2.318(4)	S(1)−Co−P	124.8(1)
	Co−S(3)	2.296(4)	S(2)−Co−P	125.3(2)
	Co−P	2.272(4)	S(3)−Co−P	122.1(2)
1-PMe$_2$Ph	Co−S(1)	2.297(1)	B···Co−P	179.0(1)
	Co−S(2)	2.305(1)	S(1)−Co−P	123.05(3)
	Co−S(3)	2.318(1)	S(2)−Co−P	125.20(3)
	Co−P	2.2570(7)	S(3)−Co−P	123.99(3)

(8) DuPont, J. A.; Coxey, M. B.; Schebler, P. J.; Incarvito, C. D.; Dougherty, W. G.; Yap, G. P. A.; Rheingold, A. L.; Riordan, C. G. *Organometallics* **2007**, *26*, 971.

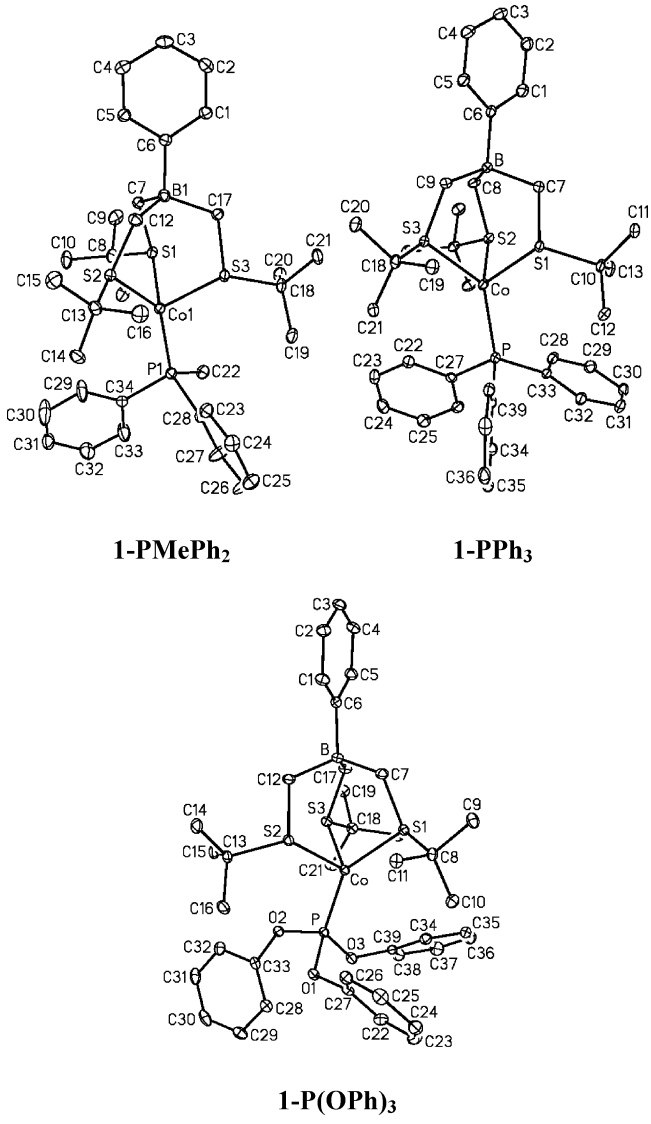

Figure 3. Thermal ellipsoid plots of **1-PMePh$_2$**, **1-PPh$_3$**, and **1-P(OPh)$_3$**. Thermal ellipsoids are drawn to 30% probability. Hydrogen atoms have been omitted for clarity.

The longer Co−S distances in the latter cobalt(II) complex are a consequence of the strong σ-donor ability of the methyl ligand. The Co−P bond distances of 2.2561(6) Å (**1-PMe$_3$**), 2.272(4) Å (**1-PEt$_3$**), and 2.2570(7) Å (**1-PMe$_2$Ph**) are similar to those of the other **1-L** analogues synthesized in this series yet do not exhibit a discernible trend (Table 3).

Id. Molecular Structures of 1-PMePh$_2$, 1-PPh$_3$, and 1-P(OPh)$_3$. Thermal ellipsoid plots of **1-PMePh$_2$**, **1-PPh$_3$**, and **1-P(OPh)$_3$** are given in Figure 3, and selected metric parameters are listed in Table 4. **1-PMePh$_2$** crystallized with two independent molecules in the asymmetric unit, only one of which is shown in Figure 3; metric parameters for each independent molecule are provided in Table 4. These complexes exhibit a clear distortion away from idealized C_3 symmetry. Specifically, the α angles equal 11.2 (average of the two independent molecules), 13.4, and 23.6° for **1-PMePh$_2$**, **1-PPh$_3$**, and **1-P(OPh)$_3$**, respectively. Necessarily, the off-axis nature of the phosphine ligand results in very different S−Co−P angles. For example, in **1-P(OPh)$_3$**, two of the S−Co−P angles are similar, measuring 110.00(2) and 105.01(2)°, while the third angle is much larger, 145.25(4)°. The Co−S bond distances are unexceptional, averaging 2.302(2), 2.310(1), and 2.321(1) Å for **1-PMe$_2$Ph**, **1-PPh$_3$**, and **1-P(OPh)$_3$**, respectively. The Co−P bond distances are 2.252(1) Å (**1-PMePh$_2$**), 2.259(9) Å (**1-PPh$_3$**), and 2.1448(6) Å [**1-P(OPh)$_3$**]. To the best of our knowledge, the Co−P bond distance in **1-P(OPh)$_3$** is much shorter than those found for any of the other cobalt(I) derivatives. The difference derives from the high π-acceptor aptitude of P(OPh)$_3$.

Table 4. Selected Metric Parameters for **1-PMePh$_2$**, **1-PPh$_3$**, and **1-P(OPh)$_3$**

		length, Å		angle, deg
1-PMePh$_2$ (1)	Co(1)−S(1)	2.322(1)	B(1)···Co(1)−P(1)	163.85(9)
	Co(1)−S(2)	2.296(1)	S(1)−Co(1)−P(1)	112.26(4)
	Co(1)−S(3)	2.313(1)	S(2)−Co(1)−P(1)	139.37(5)
	Co(1)−P(1)	2.252(1)	S(3)−Co(1)−P(1)	114.77(4)
1-PMePh$_2$ (2)	Co(2)−S(6)	2.279(1)	B(2)···Co(2)−P(2)	173.99(9)
	Co(2)−S(5)	2.298(1)	S(4)−Co(2)−P(2)	128.78(5)
	Co(2)−S(4)	2.304(1)	S(5)−Co(2)−P(2)	120.83(5)
	Co(2)−P(2)	2.268(1)	S(6)−Co(2)−P(2)	119.89(5)
1-PPh$_3$	Co−S(1)	2.2968(9)	S(1)−Co−S(2)	166.6(1)
	Co−S(2)	2.3290(9)	S(1)−Co−P	117.62(3)
	Co−S(3)	2.2962(9)	S(2)−Co−P	113.45(3)
	Co−P	2.2656(9)	S(3)−Co−P	136.30(3)
1-P(OPh)$_3$	Co−S(1)	2.3079(6)	B···Co−P	156.44(4)
	Co−S(2)	2.3366(6)	S(1)−Co−P	145.25(2)
	Co−S(3)	2.3197(6)	S(2)−Co−P	110.00(2)
	Co−P	2.1448(6)	S(3)−Co−P	105.01(2)

IIa. Synthesis and Properties of 1-CNBu^t. The addition of 1 equiv of *tert*-butyl isocyanide to a stirring diethyl ether solution of [PhTt^{tBu}]CoCl resulted in a rapid color change from blue to green. Subsequent addition of 1 equiv of a Na/Hg amalgam produced a further color change to yellow with concomitant precipitation of a white solid, NaCl. Removal of the volatiles, followed by extraction with pentane, afforded the corresponding monovalent cobalt species, **1-CNBu^t**, in 60% yield (Scheme 2). This high-spin, $S = 1$ complex is thermally stable but decomposes rapidly upon exposure to air or moisture. **1-CNBu^t** is soluble in THF, ether, and pentane. It reacts with chlorinated hydrocarbons generating [PhTt^{tBu}]CoCl.

IIb. Analysis of 1-CNBu^t: Proton NMR, Electronic Absorption, and Infrared (IR) Spectra. The proton NMR spectrum of paramagnetic **1-CNBu^t** is similar to those of the other four-coordinate **1-L** complexes studied herein as well as the [PhTt^{tBu}]Ni(CNBu^t) analogue. A broad singlet located at δ 114.5 is assigned to the six methylene protons of the borato ligand. A broad upfield resonance at δ 0.18 is ascribed to the thee equivalent *tert*-butyl groups. The *meta*, *ortho*, and *para* protons of the borato ligand are located at δ 15.3, 10.3, and 9.83, respectively. The *tert*-butyl isocyanide proton resonance, δ 12.0, is shifted downfield from free isocyanide. The triplet ground state of **1-CNBu^t** is confirmed by its magnetic moment, $\mu_{eff} = 3.1(1)\ \mu_B$.[9]

The terminal CNBu^t ligand is characterized by an intense infrared band, $\nu_{CN} = 2198\ cm^{-1}$. Coordination results in a shift to higher energy relative to free CNBu^t, $\nu_{CN} = 2142\ cm^{-1}$ ($CHCl_3$). The ν_{CN} stretch for the nickel analogue [PhTt^{tBu}]Ni(CNBu^t), $\nu_{CN} = 2115\ cm^{-1}$, in which the CNBu^t

(9) (a) Evans, D. F. *J. Chem. Soc.* **1959**, 2003. (b) Live, D. H.; Chan, S. I. *Anal. Chem.* **1970**, *42*, 791.

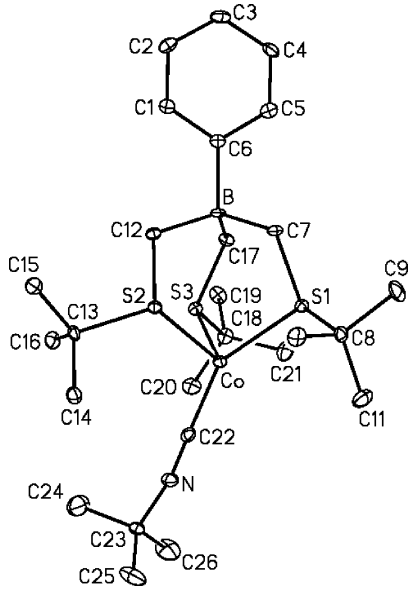

Figure 4. Thermal ellipsoid plot of **1-CNBu^t**. Thermal ellipsoids are drawn to 30% probability. Hydrogen atoms have been omitted for clarity.

ligand resides on the 3-fold axis,[10] is at a much lower energy. The d^9 nickel(I) ion participates in greater π-backbonding, when compared to the d^8 cobalt(I) ion, in part because of its higher electron count. The ν_{CN} value is higher for **1-CNBu^t** than for CNBu^t, suggesting that σ-donation predominates over π-back-donation. A secondary effect that also may increase the ν_{CN} energy is kinematic coupling of the C−N and M−C oscillators,[11] although this phenomenon cannot account fully for the differences observed here.

The electronic absorption spectrum of **1-CNBu^t** displays a single, weak d-d transition at 780 (70) nm. The expected lower-energy ligand field transitions were not observed for **1-CNBu^t** and are presumably shifted to the near-IR region beyond 1100 nm. The energy of the latter transition ranged from 718 to 905 nm in the **1-L** phosphine complexes. The similar complexes, [Tp^{Np}]Co(CO) and [(Tp^{Np})Co]$_2$(μ-N$_2$), displayed transitions at λ_{max} = 1135 and 992 nm, respectively.[5]

IIc. Molecular Structure of 1-CNBu^t. Examination of the structure of **1-CNBu^t** reveals a significant deviation from C_3 symmetry with α equaling 26.5°, the largest angle among the series of complexes reported (Figure 4 and Table 6). This structural deviation results in two similar and more acute S−Co−C bond angles of 103.5(1) and 110.1(1)° and one much more open S−Co−C(22) angle of 148.5(1)°. The Co−C bond distance of 1.857(1) Å is similar to those of other cobalt(I) isocyanide complexes. For example, [Co(CNC$_6$H$_5$)$_5$]$^+$ has Co−C bond lengths averaging 1.84(3) Å,[12] and [Co(CNCH$_3$)$_5$]$^+$ has Co−C bond lengths averaging 1.88(2) Å.[13] The distortion of the CNBu^t ligand off of the B···Co−C vector is of equal magnitude as that seen in Theopold's [Tp^{Np}]Co(CO), where α equals 26.6°. A similarly distorted structure is presumed for [PhTt^{tBu}]Co(CO), **1-CO**. This species, which is in equilibrium with the low-spin dicarbonyl [PhTt^{tBu}]Co(CO)$_2$,[8] has yet to be structurally characterized.

Table 5. Comparison of α Angles for **1-L** Complexes and Related [Tp^R]Co(L′) and [PhBP$_3$]Ni(L) Complexes

	α, deg
1-PPh$_3$	13.4(1)
1-PMe$_3$	3.4(1)
1-PEt$_3$	1.7(1)
1-PMe$_2$Ph	1.0(1)
1-PMePh$_2$	6.0(1),16.1(1),av=11.1(3)
1-P(OPh)$_3$	23.6(4)
1-CNBu^t	26.5(1)
[(Tp^{Np})Co]$_2$(μ-N$_2$)[5]	34.7,37.9
[Tp^{Np}]Co(CO)[5]	25.7
[PhBP$_3$]Ni(S-*p*-^{t}Bu-Ph)[21]	29.2

Table 6. Selected Bond Lengths (Å) and Bond Angles (deg) for **1-CNBu^t**

	length, Å		angle, deg
Co−S(1)	2.322(1)	B···Co−P (av)	153.5(1)
Co−S(2)	2.307(1)	S(1)−Co−C(22)	148.5(1)
Co−S(3)	2.314(1)	S(2)−Co−C(22)	110.1(1)
Co−C(22)	1.857(4)	S(3)−Co−C(22)	103.5(1)
C−N	1.161(5)	S(1)−Co−S(2)	93.72(4)

Table 7. Steric and Electronic Parameters of Tertiary Phosphine Ligands Used in This Investigation

ligand	cone angle (deg)	pK_a of HPR$_3^+$ (aqueous)	A$_1$ ν_{CO}, cm^{-1}
PMe$_3$	118	8.65	2064.1
PEt$_3$	132	8.69	2061.7
PMe$_2$Ph	122	6.50	2065.3
PMePh$_2$	136	4.57	2067.0
PPh$_3$	145	2.73	2068.9
P(OPh)$_3$	128	2.00	2085.0

Discussion

Cobalt Structural Distortions as a Function of Phosphine Ligand. The structural characterization of the series of [PhTt^{tBu}]Co(L) complexes permits for the examination of the correlation of the α angle with phosphine donor characteristics. Such bent geometries have been observed in other four-coordinate cobalt(I) complexes. Most notably, Theopold and Doren[5] described a similar deviation from ideal C_3 symmetry in [Tp^{Np}]Co(L) complexes (Table 5). They employed the extended Hückel molecular orbital and density functional theories to provide a detailed framework to understand the structures of [Tp^{Np}]Co(L) complexes.[5] The latter approach accurately reproduced the molecular geometries determined by X-ray diffraction analyses. By examination of complexes in the formal Co(I), Co(II), and Co(III) oxidation states, it was determined that the d^8, Co(I), configuration was necessary but not sufficient to access the bent geometry. Examination of the frontier molecular orbitals in the context of a Walsh diagram that considers bending of the L = CO ligand off-axis (i.e., reduction of the molecular symmetry from C_{3v} to C_s) proved instructive.[5] In summary, the bent geometry is ascribed to a preferred electronic structure anticipated for d^8 complexes possessing ligands that are both good σ-donors and π-acceptors. In the studies by Theopold, both L = CO and N$_2$ satisfy this requirement.

(10) Mandimutsira, B. S.; Riordan, C. G. Unpublished results.
(11) Cotton, F. A.; Zingales, F. *J. Am. Chem. Soc.* **1961**, *83*, 351.
(12) Jurnak, F. A.; Greig, D. R.; Raymond, K. N. *Inorg. Chem.* **1975**, *14*, 2585.
(13) Cotton, F. A.; Wood, J. S.; Dunne, T. G. *Inorg. Chem.* **1964**, *3*, 1495.

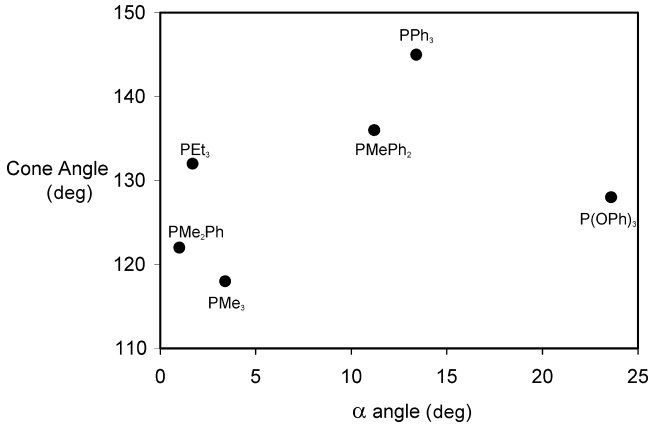

Figure 5. Plot of the Tolman cone angle versus the α angle for **1-L** complexes. The α angle was determined by X-ray diffraction.

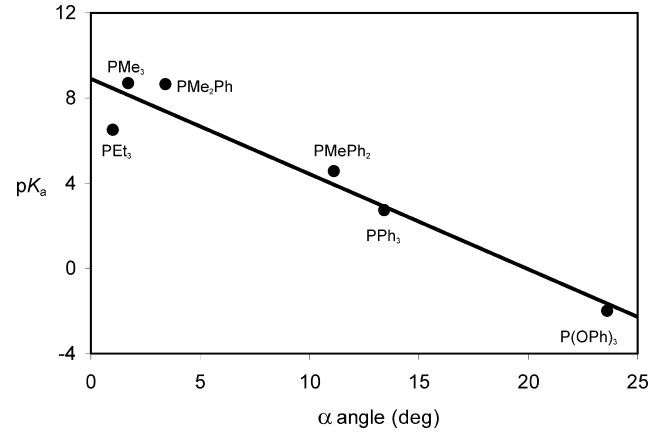

Figure 6. Plot of pK_a (of the conjugate acid of PR_3) versus α angle. The line represents a best-fit linear regression, $R^2 = 0.962$.

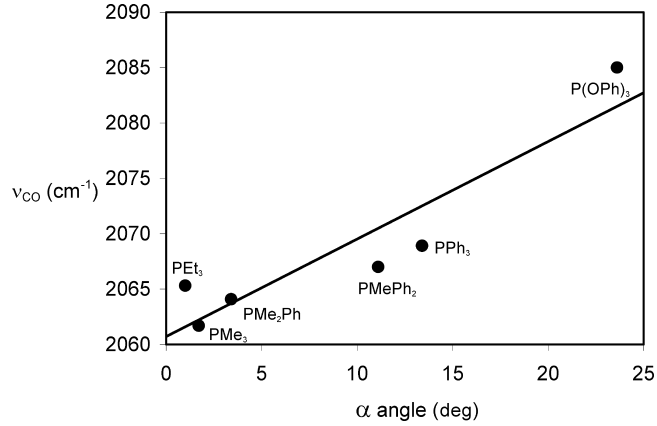

Figure 7. Plot of Tolman electronic parameter (ν_{CO}) versus α angle. The line represents a best-fit linear regression, $R^2 = 0.917$.

To further validate and extend the analysis of the structural distortions of the [Tp^{Np}]Co(L) (L = N_2, CO) complexes, we consider the structural distortions exhibited by the series of complexes, [PhTt^{tBu}]Co(L). The characteristics of the six phosphine donors employed provide a means for deducing the roles of phosphine steric and electronic effects on molecular geometry. In this context, we are unaware of phosphine derivatives of the type [Tp^R]Co(PR′$_3$). Extensive efforts by Tolman[14] and others[15] have quantified systematically the steric and electronic properties of phosphines. First, we consider phosphine sterics as measured by the Tolman cone angles (Table 7).[16] A plot of the Tolman cone angle versus the α angle (Figure 5) shows clearly that there is no correlation. For example, PEt_3 and $P(OPh)_3$ have similar cone angles, yet the α angles in **1-PEt$_3$** and **1-P(OPh)$_3$** differ by about 22°. Furthermore, PPh_3 has the largest cone angle in the series at 145°, yet **1-PPh$_3$** exhibits an α angle of 13.4°.

To explore a correlation between the electronic properties of the phosphine ligands and the α angle, we consider two different measures of the former. Henderson and Streuli[17] have measured the relative basicity of substituted phosphines by determining the pK_a values of their conjugate acids (Table 7). A plot of pK_a versus the α angle is provided in Figure 6. This plot shows that a qualitative correlation exists with a correlation coefficient of 0.962 ($p \leq 0.0022$). Specifically, the more basic phosphines lead to [PhTt^{tBu}]Co(L) complexes with small α angles, while those that are less basic lead to bent [PhTt^{tBu}]Co(L) complexes. For example, PEt_3 is the most basic phosphine examined in this study with a pK_a of 8.69, and **1-PEt$_3$** displays a small α angle of 2.0°. Conversely, the least basic donor is $P(OPh)_3$ with a pK_a of −2.00. Complex **1-P(OPh)$_3$** shows a significantly bent structure with a large α angle of 23.6°.

pK_a may not be the most appropriate measure of the electronic contribution of the phosphine ligand. These aqueous pK_a measurements are dependent upon the interactions between the phosphine and a proton, rather than the interaction between the phosphine and a polarizable metal. Furthermore, pK_a values are dependent on the solvation energies of the phosphine itself.[18] Thus, a more rigorous picture of the electronic effects of the phosphines in coordination chemistry is available by comparing the Tolman electronic parameter (ν_{CO}) to the α angles. The former values were derived via analysis of the series of complexes $Ni(CO)_3(PR_3)$ and use CO ligands to report on electron density at the metal available for back-bonding. Examination of this plot (Figure 7) establishes the correlation between ν_{CO} and the α angle with a correlation coefficient of 0.917 ($p \leq 0.011$). Specifically, phosphines with electron-donating substituents with low CO stretching frequencies yield [PhTt^{tBu}]Co(L) complexes with small α angles. PEt_3, PMe_3, and PMe_2Ph can be classified as pure σ-donating ligands with negligible π-accepting ability. Accordingly, the corresponding **1-L** complexes display small α angles of 2, 4, and 1.5°, respectively. The addition of electron-withdrawing groups increases the π-accepting aptitude of the phosphine. Thus, consistent with the arguments of Theopold and Doren,[5] $PMePh_2$ and PPh_3 lead to monovalent cobalt complexes with increasingly larger α angles of 11.1 and 13.4°. This is further

(14) Tolman, C. A. *J. Am. Chem. Soc.* **1970**, *92*, 2956.
(15) (a) Rahman, M. M.; Liu, H. Y.; Prock, A.; Giering, W. P. *Organometallics* **1987**, *6*, 650. (b) Rahman, M. M.; Liu, H. Y.; Eriks, K.; Prock, A.; Giering, W. P. *Organometallics* **1989**, *8*, 1. (c) Suresh, C. H.; Koga, N. *Inorg. Chem.* **2002**, *41*, 1573.
(16) Tolman, C. A. *J. Am. Chem. Soc.* **1970**, *92*, 2953.
(17) (a) Henderson, W. A., Jr.; Streuli, C. A. *J. Am. Chem. Soc.* **1960**, *82*, 5791. (b) Streuli, C. A. *Anal. Chem.* **1960**, *32*, 985.
(18) Meriwether, L. S.; Fiene, M. L. *J. Am. Chem. Soc.* **1959**, *81*, 4200.

highlighted by the structure of **1-P(OPh)$_3$**, containing the electron-withdrawing phosphite, which has the largest α angle of 23.6°.

Lastly, we comment on the structure of **1-CNBu^t** with an α angle of 26.5°. Isocyanides are poorer π-acceptors than CO but better π-acceptors than alkyl or aryl phosphines, approaching the π-accepting ability of PF_3. Thus, the large α angle in **1-CNBu^t** is qualitatively in accord with the conclusions regarding the cobalt(I) phosphine complexes, namely, that ligands with π-accepting ability lead to bent [PhTt^{tBu}]Co(L) complexes with correspondingly large α angles. Indeed, the structure of **1-CNBu^t** likely serves as a good model for the structure of **1-CO**, a species detected in solution, in equilibrium with **1-(CO)$_2$**, but not yet structurally authenticated.

Summary

The synthesis of a series of phosphine-ligated [PhTt^{tBu}]-Co(L) complexes revealed systematic variations in geometric structure. Detailed examination of the results confirms a correlation between the crystallographically determined α angle and the electronic properties of L as first proposed for [Tp^{Np}]Co(L).[5] Phosphines that are purely σ-donors lead to monovalent cobalt complexes with correspondingly small α angles. Phosphines with increasingly greater π-accepting capacity yield complexes with progressively larger α angles. Thus, the observed α angle can be tuned by changing the σ-donating and π-accepting properties of the ligand. Additionally, this can be further expanded to include non-phosphine ligands (e.g., CNBu^t), which are strong σ-donating and π-accepting ligands. Lastly, we note that such bent structures should be available to other metal complexes with d^8 configurations such as Ni(II) and Fe(0), which is a topic of some interest to us.

Experimental Section

General Considerations. Unless otherwise noted, all reactions were carried out under an inert atmosphere of N_2 using standard Schlenk techniques or in an Ar-filled Vacuum Atmospheres glovebox equipped with a gas purification system.[19] All glassware was dried at 140 °C for at least 4 h. Solvents were dried by passage through a column of activated alumina, followed by thorough degassing with N_2. Triphenylphosphine, triethylphosphine, and *tert*-butyl isocyanide were purchased from Acros Organics and used as received. Dimethylphenylphosphine and methyldiphenylphosphine were purchased from Strem Chemical and used as received. Trimethylphosphine was purchased from Sigma Aldrich Chemical and used as received. [PhTt^{tBu}]CoCl was prepared as described previously.[1] Deuterated solvents were purchased from Cambridge Isotope Laboratories and dried over 4 Å molecular sieves.

Proton and ^{13}C NMR spectra were recorded on either a Bruker 360 MHz spectrometer equipped with a Sun Workstation, a Bruker AM 250 MHz spectometer, or a Bruker AC 250 MHz spectrometer. All NMR signals were referenced to residual protio solvent signals. Unless otherwise noted, all data were collected at ambient temperature. Chemical shifts are quoted in δ (ppm) and coupling constants in hertz. Abbreviations are as follows: s, singlet; br, broad.

(19) Shriver, D. F.; Drezdon, M. A. *The Manipulation of Air Sensitive Compounds*, 2nd ed.; Wiley: New York, 1986.

Phosphorus NMR spectra were recorded on a Bruker 360 MHz NMR spectrometer, using an aqueous solution of 85% phosphoric acid as the external standard (0 ppm). Magnetic moments were determined in solution via the method of Evans.[9] Electronic spectra were recorded on a Hewlett-Packard 8453 diode array spectrometer. Infrared spectra were recorded on a Mattson Genesis Series Fourier transform infrared (FT-IR) spectrometer under a N_2 purge at ambient temperature. Solid-state FT-IR samples were prepared as KBr pellets, and solution-state FT-IR samples were prepared in pentane between KBr discs. Melting points were determined with a Melt-Temp melting point determination apparatus and are reported uncorrected. Elemental analyses were performed by Desert Analytics, Inc., Tucson, AZ; Galbraith Laboratory, Inc., Knoxville, TN; or Oneida Research Services, Inc., Whitesboro, NY. Crystallographic data were collected on a Bruker-AXS APEX diffractometer. All software and sources of the scattering factors are contained in various versions of the SHELXTL program library (G. Sheldrick, Siemens XRD, Madison, WI).

Synthesis of [PhTt^{tBu}]Co(L) Complexes. The preparation of **1-PPh$_3$** is described in detail below and is exemplary of the procedure employed in the synthesis of all complexes. Each reaction commenced with 100 mg of [PhTt^{tBu}]CoCl.

(i) 1-PPh$_3$. [PhTt^{tBu}]CoCl (100 mg, 0.20 mmol) was dissolved in 40 mL of diethyl ether. PPh_3 (64 mg, 0.24 mmol) was added to the mixture with vigorous stirring until the solid dissolved. One equivalent of a 0.3% Na/Hg (5 mg of Na, 1.56 g of Hg) amalgam was added to the reaction mixture and stirred, resulting in a color change from blue-green to yellow and the formation of a white precipitate, NaCl. The solution was stirred for 8−12 h. The reaction mixture was filtered through a Celite pad on a medium porosity filter frit, and the filtrate was collected. The solvent was removed under reduced pressure. The yellow product was extracted with pentane and eluted through a silica gel plug. The solvent was removed in vacuo yielding a yellow solid. Yield: 95 mg (65%). Mp: 150 °C dec. ^{1}H NMR (C_6D_6): δ 102.8 [br, 6 H, (CH_2)], 16.2 [s, 2 H, *m*-(C_6H_5)B], 10.9 [s, 2 H, *o*-(C_6H_5)B], 10.0 [s, 1 H, *p*-(C_6H_5)B], 9.76 [s, 6 H, *m*-(C_6H_5)P], 9.10 [br, 6 H, *o*-(C_6H_5)P], 6.88 [s, 3 H, *p*-(C_6H_5)P], 0.43 [br, 27 H, (CH_3)$_3$S]. μ_{eff} (C_6D_6) = 2.9 μ_B. UV−vis (pentane), λ_{max} (ε, M^{-1} cm^{-1}): 614 (30), 901 (596). Anal. Calcd for $C_{39}H_{53}S_3BCoP$: C, 65.2; H, 7.43. Found: C, 65.4; H, 7.16.

(ii) 1-PMe$_3$. Yield: 43 mg (40%). Mp: 120 °C dec. ^{1}H NMR (C_6D_6): δ 97.3 [br, 5 H, (CH_2)], 44.1 [br, 9 H, (PCH_3)], 15.1 [s, 2 H, *m*-(C_6H_5)B], 10.6 [s, 2 H, *o*-(C_6H_5)B], 9.57 [s, 1 H, *p*-(C_6H_5)B], 0.22 [br, 27 H, (CH_3)$_3$S]. μ_{eff} (C_6D_6) = 2.9 μ_B. UV−vis (pentane), λ_{max} (ε, M^{-1} cm^{-1}): 686 (74), 893 (314). Anal. Calcd for $C_{24}H_{47}S_3BCoP$: C, 54.1; H, 8.89. Found: C, 53.6; H, 8.54.

(iii) 1-PEt$_3$. Yield: 50 mg (43%). Mp: 140 °C dec. ^{1}H NMR (C_6D_6): δ 95.4 [br, 6 H, (CH_2)], 18.9 [br, 5 H, (PCH_2CH_3)], 16.2 [s, 2 H, *m*-(C_6H_5)B], 11.0 [s, 2 H, *o*-(C_6H_5)B], 9.91 [s, 1 H, *p*-(C_6H_5)B], 4.02 [br, 9 H, (PCH_2CH_3)], 0.60 [br, 27 H, (CH_3)$_3$S]. μ_{eff} (C_6D_6) = 3.0 μ_B. UV−vis (pentane), λ_{max} (ε, M^{-1} cm^{-1}): 711 (135), 905 (671). Anal. Calcd for $C_{27}H_{53}S_3BCoP$: C, 60.8; H, 8.90. Found: C, 60.2; H, 9.01.

(iv) 1-PMe$_2$Ph. Yield: 68 mg (57%). Mp: 143 °C dec. ^{1}H NMR (C_6D_6): δ 100.8 (br, 5 H, BCH_2), 48.6 (br, 5 H, PCH_3), 16.6 [s, 2 H, *m*-(C_6H_5)B], 11.3 [s, 2 H, *o*-(C_6H_5)P], 10.8 [s, 2 H, *o*-(C_6H_5)B], 9.74 [s, 1 H, *p*-(C_6H_5)B], 9.00 [s, 1 H, *p*-(C_6H_5)P], 7.26 [s, 2 H, *p*-(C_6H_5)P], 0.36 [br, 27 H, (CH_3)$_3$S]. μ_{eff} (C_6D_6) = 3.1 μ_B. UV−vis (pentane), λ_{max} (ε, M^{-1} cm^{-1}): 706 (70), 896 (508). Anal. Calcd for $C_{28}H_{49}S_3BCoP$: C, 57.4; H, 8.48. Found: C, 57.7; H, 8.04.

(v) 1-PMePh$_2$. Yield: 80 mg (60%). Mp: 147 °C dec. ^{1}H NMR (C_6D_6): δ 55.2 [br, 6 H, (CH_2)], 24.3 [s, 3 H, (PCH_3)], 15.6 [s, 4

H, *o*-(C_6H_5)P], 14.1 [s, 2 H, *m*-(C_6H_5)B], 12.1 [s, 1 H, *p*-(C_6H_5)B], 8.21 [b, 2 H, *p*-(C_6H_5)P], 7.87 [br, 2 H, *o*-(C_6H_5)B], 6.73 [s, 4 H, *m*-(C_6H_5)P], −7.51 [br, 27 H, (CH_3)$_3$S]. μ_{eff} (C_6D_6) = 2.9 μ_B. UV−vis (pentane), λ_{max} (ε, M^{-1} cm^{-1}): 710 (49), 896 (618). Anal. Calcd for $C_{34}H_{51}S_3BCoP$: C, 62.2; H, 7.83. Found: C, 62.0; H, 7.58.

(vi) 1-P(OPh)$_3$. Yield: 102 mg (66%). Mp: 135 °C dec. ^{1}H NMR (C_6D_6): δ 129.2 [br, 6 H, (CH_2)], 18.2 [s, 2 H, *m*-(C_6H_5)B], 17.9 [br, 2 H, *p*-(C_6H_5)P], 11.2 [s, 2 H, *o*-(C_6H_5)B], 10.7 [s, 1 H, *p*-(C_6H_5)B], 9.43 [br, 4 H, *m*-(C_6H_5)P], 6.60 [s, 4 H, *o*-(C_6H_5)P], −3.13 [br, 27 H, (CH_3)$_3$S]. μ_{eff} (C_6D_6) = 2.9 μ_B. UV−vis (pentane), λ_{max} (ε, M^{-1} cm^{-1}): 573 (120), 718 (257). Anal. Calcd for $C_{39}H_{53}S_3O_3BCoP$: C, 61.1; H, 6.97. Found: C, 61.2; H, 7.06.

(vii) 1-CNBu^t. Yield: 66 mg (60%). Mp: 76 °C dec. ^{1}H NMR (C_6D_6): δ 114.5 [br, 6 H, (CH_2)], 15.3 [br, 2 H, *m*-(C_6H_5)B], 12.0 [br, 9 H, (CN(CH_3)$_3$], 10.3 [br, 2 H, *m*-(C_6H_5)B], 9.84 [br, 1 H, *o*-(C_6H_5)B], 0.18 [br, 27 H, (CH_3)$_3$S]. μ_{eff} (C_6D_6) = 3.0 μ_B. UV−vis (pentane), λ_{max} (ε, M^{-1} cm^{-1}): 276 (235) 335 (192), 780 (17). IR (KBr): ν_{CN} = 2198 cm^{-1}. Anal. Calcd for $C_{26}H_{47}S_3BCoN$: C, 57.9; H, 8.78. Found: C, 57.8; H, 8.77.

X-ray Structural Solution and Refinement. Data were collected on a Bruker-AXS APEX diffractometer equipped with graphite monochromated Mo Kα radiation (λ = 0.7107 Å). The unit cell parameters and orientation matrices were determined by gathering reflections from three sets of 15−20 frames using 0.3° ω scans. No symmetry higher than triclinic was observed for **1-PMePh$_2$**, and solution in the centrosymmetric space group option yielded chemically reasonable and computationally stable results of refinement. The systematic absences in the diffraction data of the other compounds are uniquely consistent with the reported space groups. All structure factors, anomalous dispersion coefficients, and the applied SADABS absorption correction program are contained in various versions (5.1−6.12) of the SHELXTL program library.[20] All non-hydrogen atoms were anisotropically refined using the conventional full-matrix least-squares method. All hydrogen atoms were treated as idealized contributions. The CIFs are available from the Cambridge Crystallographic Data Center under the depository numbers CCDC 671800−671806.

(20) Sheldrick, G. M. *Acta Crystallogr., Sect. A* **2008**, *64*, 112.
(21) MacBeth, C. E.; Thomas, J. C.; Betley, T. A.; Peters, J. C. *Inorg. Chem.* **2004**, *43*, 4645.

(i) 1-PPh$_3$. Yellow, plate-like crystals were grown by slow evaporation of a concentrated pentane solution.

(ii) 1-PMe$_3$. Green plates were grown by slow evaporation of a concentrated benzene solution at ambient temperature. Three benzene solvent molecules were located co-crystallized in the asymmetric unit with two centered at inversion with a net occupancy of two benzene molecules per compound molecule.

(iii) 1-PEt$_3$. Pale-green blocks were grown by slow evaporation of a concentrated pentane solution at ambient temperature. The compound consistently deposited as poorly diffracting, laminar twins. The data representative of the best effort were obtained from a pseudomerohedral crystal twinned along the unique monoclinic axis diffracting only to 22° θ. The phenyl group was treated as a rigid hexagon.

(iv) 1-PMe$_2$Ph. Lime-green blocks were grown by slow evaporation of a concentrated benzene solution at ambient temperature. The thioether arms are disordered with 60/40 refined site occupancies. A benzene solvent molecule is located at the inversion center and was treated as a rigid hexagon at half-occupancy.

(v) 1-PMePh$_2$. Green blocks were grown by slow evaporation of a concentrated pentane solution at ambient temperature. Two symmetry unique but chemically equivalent molecules are located in the asymmetric unit.

(vi) 1-P(OPh)$_3$. Dark blue blocks were grown by slow evaporation of a concentrated pentane solution at ambient temperature.

(vii) 1-CNBu^t. Yellow plates were grown by slow evaporation of a concentrated pentane solution at ambient temperature. The methyl carbon atoms of the CNBu^t ligand display unresolvable rotational disorder, and rigid bond restraints were applied.

Acknowledgment. William G. Dougherty, Jr. is thanked for solving the structures of **1-PMePh$_2$** and **1-P(OPh)$_3$**. These studies were supported through funding provided by the National Science Foundation (CHE-0213260 and CHE-0518508).

Supporting Information Available: CIF files for all X-ray structures. This material is available free of charge via the Internet at http://pubs.acs.org.

IC800813U